Supplementary Materials

Highly efficient determination of Mn^{2+} in Chinese liquor by a novel electrochemical sensor based on TiO_2-NH_2@covalent organic frameworks nanocomposites

Liangyun Yu[a], Liangju Sun[a], Qi Zhang[b,*], Jingjing Zhang[a], Bairen Yang[b], Mingquan Huang[a], Yawen Zhou[a], Baocai Xu[a,*], Xiaoya Hu[c,*]

[a] *School of Light Industry, Beijing Technology and Business University, No. 11 Fucheng Road, Haidian District, Beijing 100048, P. R. China*

[b] *School of Environmental Science and Engineering, Yancheng Institute of Technology, Yancheng, 224051, P. R. China*

[c] *College of Chemistry and Engineering, Yangzhou University, 88 South University Avenue, Yangzhou 225002, P. R. China*

** Corresponding author. Tel.: +86-514-87972034.*

E-mail address: zhqisir@163.com (Q. Zhang), xubac@163.com (B.C. Xu), xyhu@yzu.edu.cn (X.Y. Hu).

Fig. S1(A–D) respectively demonstrates the TEM images of TiO_2, TiO_2-NH_2, TiO_2-NH_2@COF_{DPTB} and COF_{DPTB}. As it shown, the first three materials all exhibited the aggregation of nanoparticles, in which the aggregation degree of TiO_2-NH_2@COF_{DPTB} was significantly reduced and some pores were distributed, being consistent with the SEM characterization above.

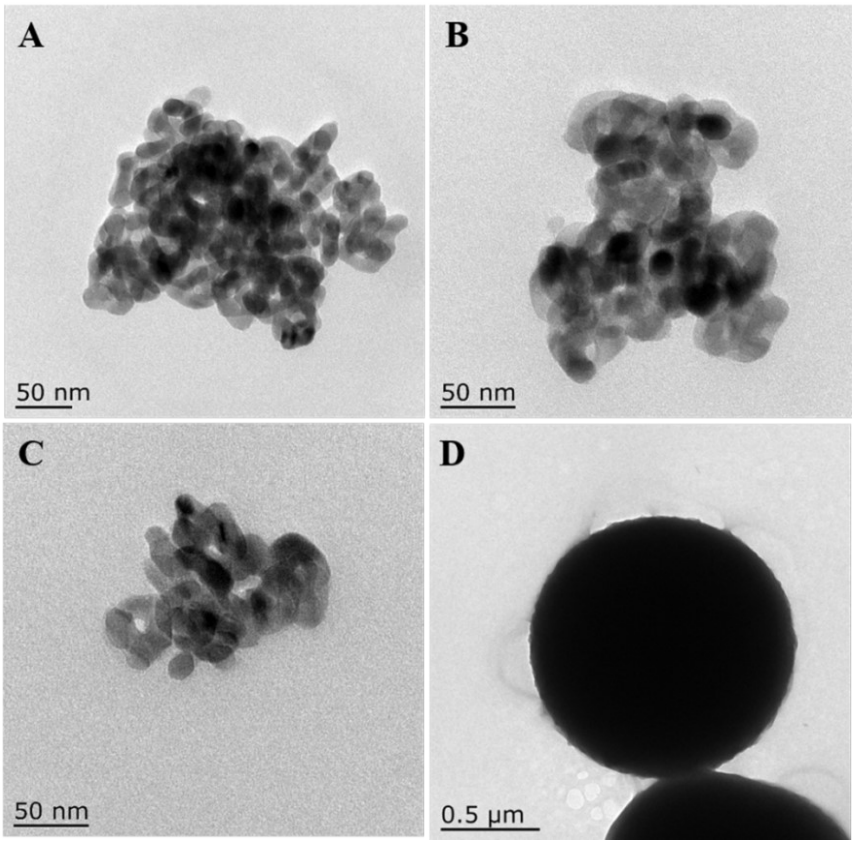

Fig. S1 TEM images of (A) TiO_2, (B) TiO_2-NH_2, (C) TiO_2-NH_2@COF_{DPTB} and (D) COF_{DPTB}.

XRD was employed for the phase and structure characterization of the nanomaterials involved. The typical XRD patterns of pure TiO_2, TiO_2-NH_2, COF_{DPTB}, and TiO_2-NH_2@COF_{DPTB} nanocomposites were illustrated in Fig. S2(A). In the top curve (a), the peaks located at 2θ=25.17°, 37.69°, 47.92°, 53.81°, 54.94°, 62.53°, 68.72°, 70.25° and 74.99° can be indexed to (101), (004), (200), (105), (211), (204),

(116), (220) and (215) of the anatase crystals of TiO_2 (JCPDS card no. 21-1272) [1, 2]. After reaction with APS, the crystal structure of TiO_2 remained unchanged (curve (b)). As can be seen in curve (c), the presence of characteristic diffraction peaks at 5.63°, 15.23°, 29.01°, and 42.42° were attributed to the crystalline COF_{DPTB}. The rest of peaks in the TiO_2-NH_2@COF_{DPTB} (curve (d)) agreed with the simulated XRD patterns of anatase TiO_2. These results revealed that COF_{DPTB} layer has indeed been coated on TiO_2-NH_2 nanoparticles. Additionally, both previous EDX (Fig. (3C)) and subsequent FTIR (Fig. S2B) analyses confirmed explicitly COF_{DPTB} existence in the composites.

To chemically bond TiO_2 onto the surface of COF_{DPTB}, it was first functionalized with amino groups by APS. Then TiO_2-NH_2@COF_{DPTB} nanocomposites were synthesized by in-situ growth of COF_{DPTB} on TiO_2-NH_2 surface using DMTP and TAPB as the starting materials based on monomer mediated growth strategy. The functional groups of TiO_2, TiO_2-NH_2, COF_{DPTB}, DMTP, TAPB and TiO_2-NH_2@COF_{DPTB} were further investigated by FTIR (Fig. S2B). As for pristine TiO_2 (curve (a)), the large and wide FTIR peak appeared at around 3278 cm^{-1} was originated from the –OH stretching vibration on the surface, demonstrating the presence of moisture [3]. The broad band below 1000 cm^{-1} can be attributed to the vibration absorbance of Ti–O–Ti, which were almost unchanged after amination (curve (b)) [3, 4]. With amino grafting to TiO_2 surface, new bands appeared in 2928, 1124 and 1062 cm^{-1}, which were ascribed to the stretching vibrations of C–H, C–N, and Ti–O–Si, respectively [5]. Moreover, the characteristic bands at 1620 and 1470 cm^{-1} can be assigned respectively to the bending modes of N–H in $–NH_2$ and the C–H

in –CH_2– [1, 6]. So, it can be confirmed that –NH_2 groups have been grafted successfully onto the surface of TiO_2 by APS. Compared to the two monomers of DMTP and TAPB, the FTIR spectroscopy (curve (c)) of pure COF_{DPTB} presented a new characteristic peak at 1615 cm^{-1}, corresponding to the stretching vibration of C=N [7]. Meanwhile, the peaks at 3433, 3354, and 3209 cm^{-1} associated with the stretching vibration of N-H in TAPB, as well as that peak at 1679 cm^{-1} of the stretching vibration of C=O in DMTP all vanished [8]. Hence, these data demonstrated that amino groups condensed successfully with aldehyde groups via the Schiff-base reaction to form the imine bonds. As curve (f) shown, the emergence of TiO_2-NH_2 in the TiO_2-NH_2@COF_{DPTB} nanocomposite was determined by the appearance of the vibration absorbance of Ti–O–Si at 1053 cm^{-1} and the large broad peak of Ti–O–Ti below 1000 cm^{-1}, while other characteristic peaks of COF_{DPTB} remain retained. In summary, FTIR spectra suggested the generation of TiO_2-NH_2@COF_{DPTB}, which was consistent with the above results.

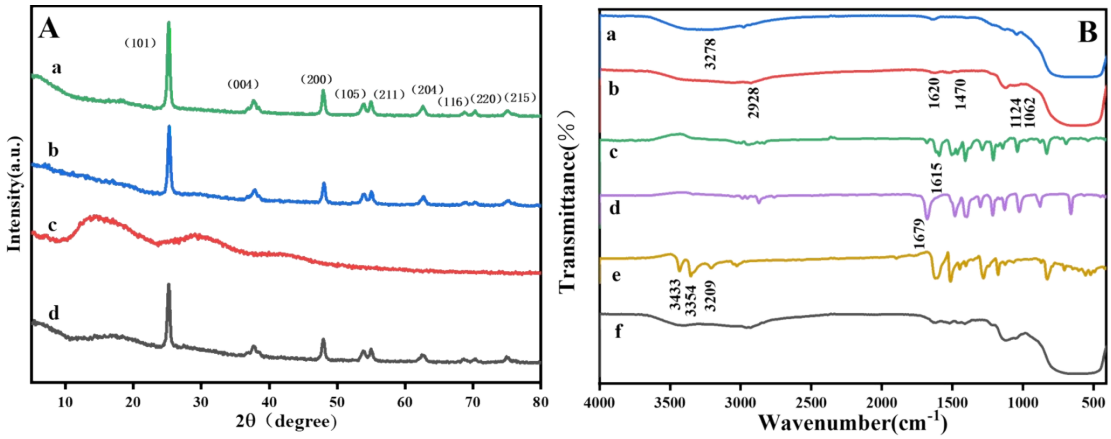

Fig. S2 (A) XRD patterns of (a) TiO_2, (b) TiO_2-NH_2, (c) COF_{DPTB}, and (d) TiO_2-NH_2@COF_{DPTB}. (B) FTIR spectra of (a) TiO_2, (b) TiO_2-NH_2, (c) COF_{DPTB}, (d) DMTP, (e) TAPB, and (f) TiO_2-NH_2@COF_{DPTB}.

Analytical parameters optimization

To obtain the best detection of Mn^{2+} based on TiO_2-NH_2@COF_{DPTB}/GCE, the concentration of TiO_2-NH_2@COF_{DPTB}, the pH value of NH_3-NH_4Cl buffer, the deposition potential and deposition time, as well as the SDS concentration were optimized, and the results were shown in Fig. S3. It should be noted that, most of the time, double reduction peaks were observed during the cathodic scan, indicating that the reduction went through an intermediate state of Mn (III) [9, 10]. And with the increase of Mn^{2+} concentration (≥8.0 nm), the bimodal was more obvious. This phenomenon had also been reported in the literature [9, 11]. Moreover, double stripping peaks are common to occur on solid electrodes because the stripping of the bulk portion of the deposited analyte occurs at a different potential than the stripping of the first monolayer on the electrode [9]. Considering the complexity of the peak shape, we used the peak area (charge) rather than the amplitude of peak height in the waveform analysis because the former was easier to quantify and had better linearity.

The concentration of TiO_2-NH_2@COF_{DPTB} in a range of 0.6−1.8 $mg \cdot mL^{-1}$ was optimized by SWCSV, and the result was shown in Fig. S3(A). It can be seen that the peak area increased gradually as the TiO_2-NH_2@COF_{DPTB} concentration increased. This was because as the TiO_2-NH_2@COF_{DPTB} concentration increased, that means, the composite amount on electrode surface increased, the synergistic effect and the number of binding sites increased consequently. However, when the concentration continued to increase to exceed 1.0 $mg \cdot mL^{-1}$, the modification layer on the electrode surface thickened which decreased the mass transfer ability, so the peak area

decreased instead. Hence, 1.0 $mg \cdot mL^{-1}$ was chosen as the optimum TiO_2-NH_2@COF_{DPTB} concentration in the subsequent measurements.

As shown in previous equations (1) and (2), the redox of Mn^{2+} is dependent on pH. So, to further explore the electrochemical properties of TiO_2-NH_2@COF_{DPTB}/GCE, the influence of buffer pH on the stripping signal was investigated in 0.05 M NH_3-NH_4Cl buffer. Our results showed that when pH was less than 8.0, the peak deformation was serious and the response current can't be accurately read. Moreover, the stronger the acidity, the smaller the peak current and the more severe the deformation of the peak shape. Thus, the effect of pH in the 8.5−10.5 range on the modified electrode was studied. As the results in Fig. S3(B) demonstrated, the largest peak area with good looking peak shape was obtained around pH 9.0. At higher pH values, the decrease in peak area was because of the inadequate solubility of Mn^{2+} in more basic pH for the increase of the competitive product $Mn(OH)_2$, which can then be oxidized by dissolved O_2 in the solution to precipitate $Mn(OH)_4$ [12]. It was also found that the cathodic reduction potential shifted in the more negative direction as pH increased, possibly due to the reduced proton mass transfer to the interface electrode surface/deposition [13]. Therefore, the subsequent experiments involved NH_3-NH_4Cl buffer with pH 9.0.

Next, we optimized the SWCSV step based on the fact that the pre-concentration step is critical to any stripping technique. First of all, the effect of deposition potential on the SWCSV responses was examined by varying it from 0.3−0.7 V with intervals of 0.1 V. As revealed in Fig. S3(C), the potential of 0.3 V was too negative to

maximize the oxidation of Mn^{2+}, thus the reduction peak area of MnO_2 was almost zero [14]. The peak area first increased with the cathodic scanning potential continued to increase, and then decreased as it more positive than 0.5 V. In addition, the peak shape was also the best at 0.5 V deposited potential. Accordingly, 0.5 V was used as the optimum potential for production sufficient quantities of MnO_2 for detection in the following experiments.

Fig. S3(D) assessed the effect of deposition time varied by 50 s from 450 to 650 s on the sensitivity to find the minimum time for sufficient sensitivity. As is shown, the peak area increased sharply with the increase of accumulation time from 450 to 550 s, and then gradually decreased after it exceeded 550 s, indicating that the deposition of manganese oxide on the electrode surface had reached saturation. Thus, the deposition time of 550 s was chosen for subsequent studies.

Surfactants are one kind of amphiphilic ions or molecules with a hydrophilic head at one end and a long hydrophobic tail at the other, and have been widely used in the field of electrochemistry and electroanalytical chemistry due to their ability to enhance and improve the electrode/solution interface properties by adsorption at the interfaces or aggregation into supramolecular structures [15]. SDS, as an anion surfactant, its negatively charged layer can adsorb positively charged Mn^{2+} to the electrode surface through electrostatic interaction, reduce the electrode reaction overvoltage and accelerate the electron transfer rate. Besides, Mn^{2+} in the solution may also form a transient adduct with SDS, which is likely to be adsorbed on the surface of electrode, making the electron transfer reaction of Mn^{2+} easier to take place.

So the anionic surfactant SDS should effectively promote the electrochemical responses of Mn^{2+}, which was proved in Fig. S3(E). It can be seen that the maximum enhancement of the current response was achieved when the SDS concentration was 1.0 mM, which was used as its application concentration in the subsequent experiments.

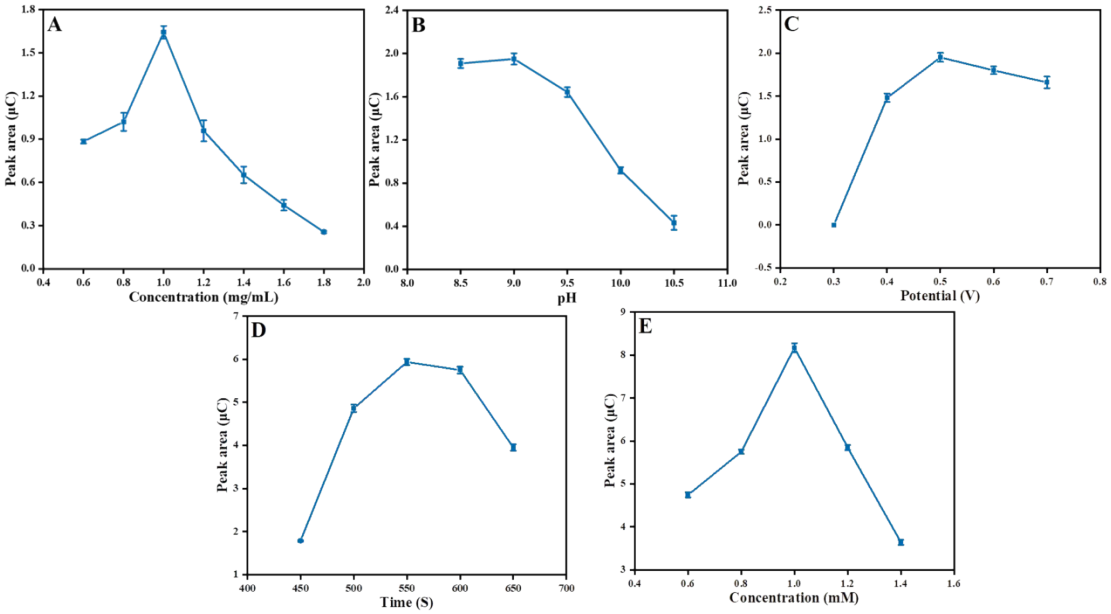

Fig. S3 The effects of (A) the concentration of TiO_2-NH_2@COF_{DPTB}**,** (B) the pH value of NH_3-NH_4Cl buffer, (C) the deposition potential, (D) the deposition time, and (E) the concentration of SDS on the cathodic stripping signal. Error bars are the standard error of the mean (n=6).

References

[1] M.M. Kang, M.H. Wang, S. Zhang, X.D. Dong, L.H. He, Y.H. Zhang, D.J. Guo, P.Y. Wang, S.M. Fang, Z.H. Zhang, *Electrochim. Acta*, 2015, **161**, 186-194.

[2] Q. Zhang, L.Y. Yu, C.C. Xu, W. Zhang, M. Chen, Q. Xu, G.W. Diao, *Chem. Phys. Lett.*, 2020, **761**, 138073.

[3] F. Vajedi, H. Dehghani, *Mater. Sci. Eng. B*, 2019, **243**, 189-198.

[4] H.F. Zhang, S.M. Shuang, G.Z. Wang, Y.J. Guo, X.L. Tong, P. Yang, A.J. Chen, C. Dong, Y. Qin, *RSC Adv.*, 2015, **5**, 4343-4349.

[5] K. Jiang, J. Zhang, Y.F. Wan, Z.J. Liu, J.W. Chen, *Opt. Mater.*, 2021, **114**, 110913.

[6] F.M. Liu, Y. Zhang, W. Yin, C.J. Hou, D.Q. Huo, B. He, L.L. Qian, H.B. Fa, *Sens. Actuators B Chem.*, 2017, **242**, 889-896.

[7] Y. Xie, T. Zhang, Y.L. Chen, Y. Wang, L. Wang, *Talanta*, 2020, **213**, 120843.

[8] X. Sun, N. Wang, Y. Xie, H.C. Chu, Y. Wang, Y. Wang, *Talanta*, 2021, **225**, 22072.

[9] W.J. Kang, C. Rusinek, A. Bange, E. Haynes, W.R. Heineman, I. Papautsky, *Electroanalysis*, 2017, **29**, 686-695.

[10] S. Nijjer, J. Thonstad, G.M. Haarberg, *Electrochim. Acta*, 2000, **46**, 395-399.

[11] E. Boselli, Z.Z. Wu, A. Friedman, B.C. Henn, I. Papautsky, *Environ. Sci. Technol.*, 2021, **55**, 7501-7509.

[12] J.W. Di, F. Zhang, *Talanta,* 2003, **60**, 31-36.

[13] W.J. Kang, X. Pei, A. Bange, E.N. Haynes, W.R. Heineman, I. Papautsky, *Anal. Chem.*, 2014, **86**, 12070-12077.

[14] P.P. Xie, X.X. Chen, F. Wang, C.G. Hu, S.S. Hu, *Colloids Surf., B*, 2006, **48**, 17-23.